Bridging Methylene to Bridging Acyl Conversion in Heterobinuclear Rh/Ru Complexes: Models for Adjacent-Metal Involvement in Bimetallic Catalysts

Bryan D. Rowsell, Robert McDonald,[†] and Martin Cowie*

Department of Chemistry, University of Alberta, Edmonton, Alberta, Canada T6G 2G2

Protonation of the methylene-bridged complex [RhRu(CO)$_4$(μ-CH$_2$)(dppm)$_2$][CF$_3$SO$_3$] (**1**) at −80 °C yields an asymmetrically bridged methyl complex in which the methyl ligand is σ-bound to Ru while being involved in an agostic interaction with Rh. Warming to −40 °C results in migration of the methyl group to a terminal site on Rh, and further warming to 0 °C results in migratory insertion to give the acetyl-bridged complex [RhRu(OSO$_2$CF$_3$)-(CO)$_2$(μ-C(CH$_3$)O)(μ-CO)(dppm)$_2$][CF$_3$SO$_3$] (**4**), in which the acetyl carbon is bound to Rh and its oxygen is bound to Ru. At ambient temperature one carbonyl is lost from **4** to give [RhRu-(OSO$_2$CF$_3$)(CO)$_2$(μ-C(CH$_3$)O)(dppm)$_2$][CF$_3$SO$_3$] (**5**). Carbon-13 NMR spectroscopy and the X-ray structures of both acetyl-bridged products suggest significant carbene character in the acyl carbon. Attempts to obtain methyl and subsequently acetyl species by methylene insertion into metal−hydride bonds of the appropriate precursors [RhRu(X)(CO)$_4$(μ-H)-(dppm)$_2$][X] (X$^-$ = CF$_3$SO$_3^-$, BF$_4^-$) failed, with these hydride species being unreactive to CH$_2$N$_2$. Similarly, reaction of **1** with HCl yielded only the methyl complex [RhRu(CH$_3$)(CO)$_3$-(μ-Cl)(dppm)$_2$][CF$_3$SO$_3$], which did not undergo migratory insertion. Protonation of the methylene-bridged PMe$_3$ adduct [RhRu(PMe$_3$)(CO)$_3$(μ-CH$_2$)(dppm)$_2$][CF$_3$SO$_3$] yields [Rh*Ru*-(OSO$_2$CF$_3$)(CO)$_2$(μ-*C*(CH$_3$)O)(dppm)$_2$][CF$_3$SO$_3$] in which the binding of the acetyl group is reversed, being C-bound to Ru and O-bound to Rh. This species undergoes facile rearrangement to **5** at ambient temperature.

Introduction

Migratory-insertion reactions involving alkyl and carbonyl groups[1] are of fundamental importance in a number of catalytic processes, including olefin hydroformylation[1a,2] and methanol carbonylation,[1a,3] and may also play a role in the formation of oxygenate products in Fischer−Tropsch (FT) chemistry.[4] In the first two processes, which are based on homogeneous catalysts, the majority of studies have been carried out using monometallic complexes.[2,3] However, there has been increasing interest recently in the use of both homobinuclear[5] and heterobinuclear[6,7] complexes in which

cooperativity effects of the adjacent metals have been implicated. Although the FT process is based on heterogeneous catalysts, here again the proximity of adjacent metal sites on the catalyst surface suggests an involvement of adjacent metals in the catalytic processes.[8] In addition, in parallel to the recent emphasis on mixed-metal homogeneous catalysts noted above, the use of bimetallic FT catalysts has been probed in attempts to improve both turnover rate and selectivity.[4b−d,9]

In the majority of studies involving mixed-metal catalysts (either homogeneous or heterogeneous), little

* To whom correspondence should be addressed. E-mail: martin.cowie@ualberta.ca.
† X-ray Crystallography Laboratory.
(1) (a) Collman, J. P.; Hegedus, L. S.; Norton, J. R.; Finke, R. G. *Principles and Applications of Organotransition Metal Chemistry*; University Science Books, Mill Valley, CA, 1987; Chapter 12. (b) Niu, S.; Hall, M. B. *Chem. Rev.* **2000**, *100*, 353.
(2) (a) Pruett, R. L. *Adv. Organomet. Chem.* **1979**, *17*, 1. (b) Pruett, R. L. *J. Chem. Educ.* **1986**, *63*, 196. (c) Trzeciak, A. M.; Ziólkowski, J. J. *Coord. Chem. Rev.* **1999**, *190−192*, 883.
(3) (a) Forster, D. *Adv. Organomet. Chem.* **1979**, *17*, 255. (b) Forster, D.; Dekleva, T. W. *J. Chem. Educ.* **1986**, *63*, 205. (c) Dekleva, T. W.; Forster, D. *Adv. Catal.* **1986**, *34*, 81. (d) Maitlis, P. M.; Haynes, A.; Sunley, G. J.; Howard, M. J. *J. Chem. Soc., Dalton Trans.* **1996**, 2187. (e) *Chem. Br.* **1996**, *32*, 7. (f) *Chem. Ind. (London)* **1996**, 483.
(4) (a) Watson, P. R.; Somorjai, G. A. *J. Catal.* **1981**, *72*, 347. (b) Fukushima, T.; Arakawa, H.; Ichikawa, M. *J. Phys. Chem.* **1985**, *89*, 4440. (c) Fukushima, T.; Arakawa, H.; Ichikawa, M. *J. Chem. Soc., Chem. Commun.* **1985**, 729. (d) Ichikawa, M. *Polyhedron* **1988**, *7*, 2351. (e) Schulz, H. *Appl. Catal. A: Gen.* **1999**, *186*, 4. (f) Overett, M. J.; Hill, R. O.; Moss, J. R. *Coord. Chem. Rev.* **2000**, *206−207*, 581.

(5) (a) Broussard, M. E.; Juma, B.; Train, S. G.; Peng, W.-J.; Laneman, S. A.; Stanley, G. G. *Science* **1993**, *260*, 1784. (b) Matthews, R. C.; Howell, D. K.; Peng, W.-J.; Train, S. G.; Treleaver, W. D.; Stanley, G. G. *Angew. Chem., Int. Ed. Engl.* **1996**, *35*, 2253.
(6) (a) Hidai, M.; Orisaku, M.; Ue, M.; Koyasu, Y.; Uchida, Y. *Organometallics* **1983**, *2*, 292. (b) Hidai, M.; Fukuoka, A.; Koyasu, Y.; Uchida, Y. *J. Mol. Catal.* **1986**, *35*, 29. (c) Fukuoka, A.; Fukagawa, S.; Hirano, M.; Komiya, S. *Chem. Lett.* **1997**, 377. (d) Ishii, Y.; Miyashita, K.; Kamita, K.; Hidai, M. *J. Am. Chem. Soc.* **1997**, *119*, 6448. (e) Trzeciak, A. M.; Ziolkowski, J. J. *Coord. Chem. Rev.* **1999**, *190−192*, 883. (f) Komiya, S.; Yasuda, T.; Hirano, A.; Fukuoka, M. *J. Mol. Catal. A: Chem.* **2000**, *159*, 63. (g) Ishii, Y.; Hidai, M. *Catal. Today* **2001**, *66*, 53. (h) Rida, M. A.; Smith, A. K. *J. Mol. Catal. A: Chem.* **2002**, *202*, 87.
(7) Van den Beuken, E. K.; Feringa, B. L. *Tetrahedron* **1998**, *54*, 12985.
(8) (a) Denny, P. J.; Whan, D. A. *Catalysis (London)* **1978**, *2*, 46. (b) Walther, B. *Z. Chem.* **1989**, *29*, 117. (c) Somorjai, G. A. *Perspect. Catal.* **1992**, 147. (d) Shriver, D. F. *J. Cluster Sci.* **1992**, *3*, 459. (e) Somorjai, G. A. *Prog. Surf. Sci.* **1995**, *50*, 30. (f) George, S. M. *Chem. Rev.* **1995**, *95*, 475.
(9) Iglesia, E.; Soled, S. L.; Fiato, R. A.; Via, G. H. *J. Catal.* **1993**, *143*, 345.

Table 1. Spectroscopic Data for the Compounds

compd	IR (cm^{-1})[a–c]	NMR[d,e] (ppm)		
		^{31}P{^{1}H}[f]	^{1}H[g,h]	^{13}C{^{1}H}[h,i]
[RhRu(CO)$_4$(μ-CH$_3$)(dppm)$_2$]-[CF$_3$SO$_3$]$_2$ (**2**)		24.2 (dm), 20.8 (m)	4.10 (m, 2H), 3.63 (m, 2H), 0.30 (s, br, 3H)	219.5 (m, 1C), 190.4 (m, 1C), 187.7 (m, 1C), 183.4 (dt, $^1J_{RhC}$ = 79 Hz, $^2J_{PC}$ = 15 Hz, 1C)
[RhRu(CH$_3$)(CO)$_4$(dppm)$_2$]-[CF$_3$SO$_3$]$_2$ (**3**)		28.7 (dm), 23.0 (m)	3.41 (m, 4H), 1.66 (td, $^3J_{PH}$ = 8 Hz, $^2J_{RhH}$ = 4 Hz, 3H)	221.6 (m, br, 2C), 186.3 (m, br, 2C)
[RhRu(OSO$_2$CF$_3$)(CO)$_3$(μ-C(CH$_3$)O)-(dppm)$_2$][CF$_3$SO$_3$] (**4**)	2090 (m), 2016 (s), 1732 (m)	21.9 (s, br), 6.8 (d, br)	3.30 (m, 2H), 3.22 (m, 2H), 2.03 (s, 3H)	304.8 (dm, $^1J_{RhC}$ = 38 Hz, 1C), 250.3 (m, 1C), 196.6 (m, 1C), 184.9 (m, 1C)
[RhRu(OSO$_2$CF$_3$)(CO)$_2$(μ-C(CH$_3$)O)-(dppm)$_2$][CF$_3$SO$_3$] (**5**)	2045 (s), 1989(s)	20.8 (m), 16.9 (dm)	3.64 (m, 2H), 2.59 (m, 2H), 1.99 (s, br, 3H)	270.3 (dm, $^1J_{RhC}$ = 33 Hz, 1C), 204.2 (m, 1C), 180.4 (m, 1C)
[Rh*Ru*(OSO$_2$CF$_3$)(CO)$_2$(μ-*C*(CH$_3$)O)-(dppm)$_2$][CF$_3$SO$_3$] (**6**)	2015 (s), 1956 (s)	22.7 (m), 17.6 (dm)	3.77 (m, 2H), 3.32 (m, 2H), 1.93 (s, br, 3H)	293.3 (s, br, 1C), 196.3 (t, $^2J_{PC}$ = 14 Hz), 186.8 (dt, $^1J_{RhC}$ = 75 Hz, $^2J_{PC}$ = 14 Hz, 1C)
[RhRu(OSO$_2$CF$_3$)(CO)$_4$(μ-H)-(dppm)$_2$][CF$_3$SO$_3$] (**7a**)	2072 (m), 2040 (s), 1999 (m), 1880 (m)	27.3 (m), 25.1 (m)	5.07 (m, 2H), 3.79 (m, 2H), −10.41 (m, 1H)	
[RhRu(BF$_4$)(CO)$_4$(μ-H)(dppm)$_2$]-[BF$_4$] (**7b**)		27.1 (om)	4.52 (m, 2H), 3.81 (m, 2H), −11.07 (m, 1H)	
[RhRu(CH$_3$)(CO)$_2$(μ-Cl)(μ-CO)-(dppm)$_2$][CF$_3$SO$_3$] (**8a**)	2013 (s), 1986 (s), 1711 (m)	29.0 (m), 23.0 (dm)	4.12 (m, 2H), 3.32 (m, 2H), −0.21 (t, $^3J_{PH}$ = 6 Hz, 3H)	246.4 (m, 1C), 199.4 (t, $^2J_{PC}$ = 12 Hz, 1C), 188.8 (dt, $^1J_{RhC}$ = 76 Hz, $^2J_{PC}$ = 13 Hz, 1C)

[a] IR abbreviations: s = strong, m = medium, w = weak, sh = shoulder. [b] CH$_2$Cl$_2$ solutions unless otherwise stated, in units of cm^{-1}. [c] Carbonyl stretches unless otherwise noted. [d] NMR abbreviations: s = singlet, d = doublet, t = triplet, m = multiplet, cm = complex multiplet, dm = doublet of multiplets, om = overlapping multiplets, br = broad, dt = doublet of triplets, td = triplet of doublets, dpq = doublet of pseudo quintets. [e] NMR data at 25 °C in CD$_2$Cl$_2$ unless otherwise stated. [f] ^{31}P chemical shifts referenced to external 85% H$_3$PO$_4$. [g] Chemical shifts for the phenyl hydrogens are not given. [h] ^{1}H and ^{13}C chemical shifts referenced to TMS. [i] ^{13}C{^{1}H} NMR performed with ^{13}CO enrichment.

is understood about the roles of the different metals in the processes under study. To this end, we have been studying well-defined, heterobinuclear complexes as models for bimetallic catalysts in order to probe the roles of the different metals in fundamental processes such as carbon−carbon bond formation,[10] carbon−hydrogen bond activation,[11] migratory insertion,[12] oxidative addition,[13] and reductive elimination.[14] The study reported herein examines the roles of the different metals in the conversion of a bridging methylene group to a bridging acetyl group at a Rh/Ru core.

Experimental Section

General Comments. All solvents were dried (using appropriate desiccants), distilled before use, and stored under a dinitrogen atmosphere. Reactions were performed under an argon atmosphere using standard Schlenk techniques. Diazomethane was generated from Diazald, which was purchased

from Aldrich, as was the trimethylphosphine (1 M) solution in THF and triflic acid. The ^{13}C-enriched Diazald was purchased from Cambridge Isotopes, whereas ^{13}CO was purchased from Isotec Inc. The ^{1}H, ^{13}C{^{1}H}, and ^{31}P{^{1}H} NMR spectra were recorded on a Varian iNova-400 spectrometer operating at 399.8 MHz for ^{1}H, 161.8 MHz for ^{31}P, and 100.6 MHz for ^{13}C. Infrared spectra were obtained on a Bomem MB-100 spectrometer. Elemental analyses were performed by the microanalytical service within the department. The compounds [RhRu(CO)$_4$(dppm)$_2$][X], [RhRu(CO)$_4$(μ-CH$_2$)(dppm)$_2$][X] (**1**), and [RhRu(CO)$_3$(PMe$_3$)(μ-CH$_2$)(dppm)$_2$][CF$_3$SO$_3$] (X$^-$ = BF$_4^-$, CF$_3$SO$_3^-$; dppm = μ-Ph$_2$PCH$_2$PPh$_2$) were prepared as previously reported.[15]

Spectroscopic data for all compounds are given in Table 1.

Preparation of Compounds. (a) [RhRu(CO)$_4$(μ-CH$_3$)-(dppm)$_2$][CF$_3$SO$_3$]$_2$ (2). Triflic acid (0.70 μL, 0.0079 mmol) was added to a solution of **1** (7.1 mg, 0.0056 mmol) in 0.7 mL of CD$_2$Cl$_2$ in an NMR tube at −78 °C. No noticeable color change resulted. Compound **2** was characterized only by NMR spectroscopy, since warming the solution above −40 °C resulted in conversion to **3** and subsequent heating to ambient temperature resulted in conversion to compounds **4** and **5** (vide infra).

(b) [RhRu(CO)$_4$(μ-CH$_2$D)(dppm)$_2$][CF$_3$SO$_3$]$_2$ (2-CH$_2$D). Deuterated triflic acid (0.70 μL, 0.0079 mmol) was added to a CD$_2$Cl$_2$ solution (0.7 mL) of **1** (7.1 mg, 0.0056 mmol) in an NMR tube at −78 °C. ^{1}H NMR spectroscopy indicated a mixture of both **2** and **2**-CH$_2$D.

(c) [RhRu(CO)$_4$(μ-CD$_2$H)(dppm)$_2$][CF$_3$SO$_3$]$_2$ (2-CD$_2$H). Triflic acid (0.70 μL, 0.0079 mmol) was added to a CD$_2$Cl$_2$ solution (0.7 mL) of [RhRu(μ-CD$_2$)(CO)$_4$(dppm)$_2$][CF$_3$SO$_3$] (**1**-CD$_2$; 7.1 mg, 0.0056 mmol) in an NMR tube at −78 °C. ^{1}H NMR spectroscopy indicated a mixture of the three isotopomers **2**, **2**-CH$_2$D, and **2**-CD$_2$H.

(10) (a) Trepanier, S. J.; Sterenberg, B. T.; McDonald, R.; Cowie, M. *J. Am. Chem. Soc.* **1999**, *121*, 2613. (b) George, D. S. A.; Hilts, R. W.; McDonald, R.; Cowie, M. *Organometallics* **1999**, *18*, 5330. (c) Rowsell, B. D.; McDonald, R.; Ferguson, M. J.; Cowie, M. *Organometallics* **2003**, *22*, 2944. (d) Trepanier, S. J.; Dennett, J. N. L.; Sterenberg, B. T.; McDonald, R.; Cowie, M. *J. Am. Chem. Soc.*, in press. (e) Chokshi, A.; Rowsell, B. D.; Trepanier, S. J.; Ferguson, M. J.; Cowie, M. *Organometallics*, in press.
(11) (a) Antwi-Nsiah, F. H.; Oke, O.; Cowie, M. *Organometallics* **1996**, *15*, 506. (b) Trepanier, S. J.; Ferguson, M. J.; Cowie, M. Manuscript in preparation.
(12) (a) Wang, L.-S.; Cowie, M. *Organometallics* **1995**, *14*, 2374. (b) Antwi-Nsiah, F. H.; Oke, O.; Cowie, M. *Organometallics* **1996**, *15*, 1042. (c) Trepanier, S. J.; McDonald, R.; Cowie, M. *Organometallics* **2003**, *22*, 2638.
(13) (a) McDonald, R.; Cowie, M. *Inorg. Chem.* **1993**, *32*, 1671. (b) Wang, L. S.; McDonald, R.; Cowie, M. *Inorg. Chem.* **1994**, *33*, 3735. (c) Torkelson, J. R.; Oke, O.; Muritu, J.; McDonald, R.; Cowie, M. *Organometallics* **2000**, *19*, 854.
(14) Sterenberg, B. T.; Hilts, R. W.; Moro, G.; McDonald, R.; Cowie, M. *J. Am. Chem. Soc.* **1995**, *117*, 245.

(15) Rowsell, B. D.; Trepanier, S. J.; Lam, R.; McDonald, R.; Cowie, M. *Organometallics* **2002**, *21*, 3228.

(d) [RhRu(CO)₄(CH₃)(dppm)₂][CF₃SO₃]₂ (3). An NMR sample was prepared as described in part a. The sample was then warmed to −40 °C. Complete conversion of **2** to **3** occurred over the course of approximately 1.5 h. Compound **3** was characterized by NMR spectroscopy alone, since warming above this temperature resulted in its conversion to compounds **4** and **5**.

(e) [RhRu(OSO₂CF₃)(CO)₃(μ-C(CH₃)O)(dppm)₂][CF₃SO₃] (4). Method i. An NMR sample of compound **2** was prepared as described in part a. The sample was then warmed to 0 °C. Near total conversion of **2** to **4** occurred over the course of approximately 0.5 h.

Method ii. Compound **5** (115 mg, 0.084 mmol) was mixed with 5 mL of CH₂Cl₂ to form a bright orange slurry, over which CO was passed until the solution turned clear yellow (ca. 10 min). Dropwise addition of Et₂O (25 mL) caused the precipitation of bright yellow microcrystals. The supernatant was removed, and the crystals were washed with 2 × 5 mL of Et₂O and dried under a stream of CO, yielding 68 mg of product (58% yield). ³¹P{¹H} and ¹H NMR spectroscopy confirmed complete conversion to **4**. Anal. Calcd for C₅₇H₄₇F₆O₁₀P₄RhRuS₂: C, 48.97; H, 3.39. Found: C, 49.44; H, 3.43.

(f) [RhRu(OSO₂CF₃)(CO)₂(μ-C(CH₃)O)(dppm)₂][CF₃SO₃] (5). The compound [RhRu(CO)₄(μ-CH₂)(dppm)₂][CF₃SO₃] (**1**; 100 mg, 0.080 mmol) was dissolved in 5 mL of CH₂Cl₂. To this, at ambient temperature, was added 8.0 μL of triflic acid (0.090 mmol), and the solution was stirred for 1 h. The orange solution was concentrated under a stream of Ar to ca. 2 mL, and orange microcrystals slowly began to precipitate. Diethyl ether (20 mL) was added dropwise to the slurry. The supernatant was removed, and the crystals were washed with 2 × 15 mL of ether and dried in vacuo (72 mg, 66% yield). Anal. Calcd for C₅₆H₄₇F₆O₉P₄RhRuS₂: C, 49.10; H, 3.46. Found: C, 49.22; H, 3.45.

(g) Attempted Reaction of 5 with H₂. A Teflon-valved NMR tube was charged with 10 mg of compound **5** dissolved in 0.7 mL of CD₂Cl₂. H₂ was then passed over the solution to purge the headspace above the solution of Ar, and the container was then pressurized to ca. 1 atm of H₂. The reaction was monitored by ³¹P{¹H} NMR spectroscopy over several days, during which time the dihydride, [RhRu(CO)₃(μ-H)₂-(dppm)₂][CF₃SO₃], was detected as the only phosphorus-containing product. ¹H NMR spectroscopy showed the generation of methane.

(h) [Rh*Ru*(OSO₂CF₃)(CO)₂(μ-*C*(CH₃)O)(dppm)₂][CF₃SO₃] (6). [RhRu(PMe₃)(CO)₃(μ-CH₂)(dppm)₂][CF₃SO₃] (74 mg, 0.057 mmol) was dissolved in 10 mL of CH₂Cl₂, after which 5.5 μL (0.062 mmol) of triflic acid was added, causing an immediate color change from orange to orange-yellow. Compound **6** was characterized by NMR spectroscopy alone, since any attempt to crystallize it resulted in its conversion to **5**, yielding either mixtures of **5** and **6** or solely compound **5**.

(i) [RhRu(X)(CO)₄(μ-H)(dppm)₂][X] (X⁻ = CF₃SO₃⁻ (7a), BF₄⁻ (7b)). Although **7** was prepared with both the triflate (**7a**) and fluoborate (**7b**) anions, the synthesis described is for **7a**. The synthesis of **7b** is identical except for the use of tetrafluoroboric instead of triflic acid and the use of the BF₄⁻ salt of the precursor complex. [RhRu(CO)₄(dppm)₂][CF₃SO₃] (53 mg, 0.043 mmol) was dissolved in 10 mL of CH₂Cl₂, affording a bright yellow solution. Triflic acid was added dropwise (5.0 μL, 0.057 mmol), causing no obvious color change. The solution was stirred for 30 min, after which it was concentrated to ca. 1 mL. Dropwise addition of 15 mL of ether caused the precipitation of yellow microcrystals. The supernatant was removed, and the yellow solid was washed with 3 × 10 mL of ether and dried in vacuo (44.0 mg, 74% yield). Anal. Calcd for C₅₇H₄₇F₆O₁₀P₄RhRuS₂: C, 48.60; H, 3.28. Found: C, 48.13; H, 3.19.

(j) Attempted Reaction of 7a with CH₂N₂. A Teflon-valved NMR tube was charged with 10 mg of the compound dissolved in 0.7 mL of CD₂Cl₂. Diazomethane was then passed over the solution to purge the headspace above the solution of Ar and pressurize to ca. 1 atm of CH₂N₂. The reaction was monitored by ³¹P{¹H} NMR spectroscopy over several days, after which only **7a** was detected.

(k) [RhRu(CH₃)(CO)₂(μ-Cl)(μ-CO)(dppm)₂][X] (X⁻ = CF₃SO₃⁻ (8a), BF₄⁻ (8b)). The synthesis described for **8b** is similar to that of the triflate complex **8a**, except for starting with the BF₄⁻ salt of **1**; only the preparation of **8a** is reported in what follows. Compound **1** (76 mg, 0.061 mmol) and DMA·HCl[16] (8.2 mg, 0.067 mmol) were dissolved in 10 mL of acetone and stirred for 1 h. The yellow solution was concentrated to ca. 5 mL, to which 10 mL of ether was added dropwise, resulting in the precipitation of bright yellow crystals. The supernatant was removed, and the yellow microcrystals were washed with 2 × 10 mL of ether and dried in vacuo (68.0 mg, 89% yield). Anal. Calcd for C₅₅H₄₇ClF₃O₆P₄RhRuS: C, 52.58; H, 3.77. Found: C, 52.51; H, 3.78.

X-ray Data Collection. Orange crystals of [RhRu(OSO₂-CF₃)(CO)₃(μ-C(CH₃)O)(dppm)₂][CF₃SO₃] (**4**) were obtained by slow diffusion of diethyl ether into a nitromethane solution of the compound. Data were collected on a Bruker PLATFORM/SMART 1000 CCD diffractometer[17] using Mo Kα radiation at −80 °C and were corrected for absorption through use of the SADABS procedure. Unit cell parameters were obtained from a least-squares refinement of the setting angles of 7413 reflections from the data collection. The space group was determined to be *P2₁/n* (an alternate setting of *P2₁/c* (No. 14)). See Table 2 for a summary of crystal data and X-ray data collection information.

Red crystals of [RhRu(OSO₂CF₃)(CO)₂(μ-C(CH₃)O)(dppm)₂]-[CF₃SO₃]·2MeNO₂ (**5**) were obtained by slow diffusion of diethyl ether into a nitromethane solution of the complex. Data were collected and corrected for absorption as for compound **4** (vide supra). Unit cell parameters were obtained from a least-squares refinement of the setting angles of 5538 reflections from the data collection. The space group was determined to be *P2₁/c* (No. 14).

Yellow crystals of [RhRu(CH₃)(CO)₂(μ-Cl)(μ-CO)(dppm)₂]-[BF₄]·CH₂Cl₂ (**8b**) were obtained by slow diffusion of diethyl ether into a dichloromethane solution of the complex. Data were collected on a Bruker P4/RA/SMART 1000 CCD diffractometer using Mo Kα radiation and corrected for absorption as for **4** (vide supra). Unit cell parameters were obtained from a least-squares refinement of the setting angles of 7146 reflections from the data collection. The space group was determined to be *P2₁/n*.

Structure Solution and Refinement. The structure for **4** was solved using automated Patterson location of the heavy-metal atoms and structure expansion via the DIRDIF-96 program system.[18] Refinement was completed using the program SHELXL-93.[19] One end of one of the diphosphine ligands (involving P(3)) was found to be disordered such that the two phosphorus positions were approximately 0.2 Å apart. All attached atoms (C(51) to C(66) and attached hydrogens) were displaced over two slightly offset positions. All disordered P and C atoms were assigned equal occupancy factors and allowed to refine independently; although the disordered atoms P(3A) and P(3B) were refined anisotropically, the attached disordered carbons were refined isotropically. Hydrogen atoms were assigned positions based on the geometries of their attached carbon atoms and were given thermal parameters

(16) DMA·HCl was prepared by bubbling HCl(g) through a benzene solution of dimethylacetamide (DMA). The white solid was dried in vacuo and stored under dry argon (DMA·HCl is extremely hygroscopic).

(17) Programs for diffractometer operation, data reduction, and absorption correction were those supplied by Bruker.

(18) Beurskens, P. T.; Beurskens, G.; de Gelder, R.; Garcia-Granda, S.; Isreal, R.; Gould, R. O.; Smits, J. M. M. DIRDIF-96 Program System; Crystallography Laboratory, University of Nijmegen, Nijmegen, The Netherlands, 1996.

(19) Sheldrick, G. M. SHELXL-93: Program for Crystal Structure Determination; University of Göttingen, Göttingen, Germany, 1993.

Table 2. Crystallographic Data for Compounds 4, 5, and 8b

	[RhRu(OSO$_2$CF$_3$)(μ-C(CH$_3$)O)-(CO)$_3$(dppm)$_2$][CF$_3$SO$_3$] (**4**)	[RhRu(OSO$_2$CF$_3$)(μ-C(CH$_3$)O)(CO)$_2$-(dppm)$_2$][CF$_3$SO$_3$]·2MeNO$_2$ (**5**)	[RhRu(CH$_3$)(CO)$_2$(μ-Cl)(μ-CO)(dppm)$_2$][BF$_4$]·CH$_2$Cl$_2$ (**8b**)
formula	C$_{57}$H$_{47}$F$_6$O$_{10}$P$_4$RhRuS$_2$	C$_{58}$H$_{53}$F$_6$N$_2$O$_{13}$P$_4$RhRuS$_2$	C$_{55}$H$_{49}$BCl$_3$F$_4$O$_3$P$_4$RhRu
fw	1397.93	1492.00	1278.96
cryst dimens, mm	0.59 × 0.44 × 0.28	0.18 × 0.13 × 0.07	0.31 × 0.18 × 0.11
cryst syst	monoclinic	monoclinic	monoclinic
space group	$P2_1/n$ (alternate setting of $P2_1/c$ (No. 14))	$P2_1/c$ (No. 14)	$P2_1/n$ (alternate setting of $P2_1/c$ (No. 14))
a, Å	10.1306(5)[a]	14.8521(8)[b]	17.3516(9)[c]
b, Å	21.393(1)	24.463(1)	11.9257(6)
c, Å	26.908(1)	16.8317(9)	26.464(1)
β, deg	98.0403(8)	94.520(1)	100.251(1)
V, Å^3	5774.3(5)	6096.5(6)	5388.7(4)
Z	4	4	4
d_{calcd}, g cm^{-3}	1.608	1.626	1.576
μ, mm^{-1}	0.807	0.775	0.911
radiation (λ, Å)		graphite-monochromated Mo Kα (0.710 73)	
T, °C		−80	
scan type	ω scans (0.3°) (20 s exposures)	ω scans (0.2°) (30 s exposures)	ϕ rotations (0.3°)/ω scans (0.3°) (30 s exposures)
2θ(max), deg	52.86	52.76	52.80
no. of unique rflns	11 881 (R_{int} = 0.0191)	12 368 (R_{int} = 0.0578)	11 004 (R_{int} = 0.0573)
no of observns	10 496 ($F_o^2 \geq 2\sigma(F_o^2)$)	8659 ($F_o^2 \geq 2\sigma(F_o^2)$)	7085 ($F_o^2 \geq 2\sigma(F_o^2)$)
range of transmn factors	0.8055−0.6474	0.9478−0.8732	0.9064−0.7654
no. of data/restraints/ params	11 881 ($F_o^2 \geq -3\sigma(F_o^2)$)/0/728	12 368 ($F_o^2 \geq -3\sigma(F_o^2)$)/0/787	11 004 ($F_o^2 \geq -3\sigma(F_o^2)$)/26[d]/628
residual density, e/Å^3	1.394 to −0.635	0.936 to −0.529	1.605 to −1.272
R_1($F_o^2 \geq 2\sigma(F_o^2)$)[e]	0.0393	0.0488	0.0571
wR_2 ($F_o^2 \geq -3\sigma(F_o^2)$)[e]	0.1076	0.1083	0.1653
GOF (S)[f]	1.054 ($F_o^2 \geq -3\sigma(F_o^2)$)	1.011 ($F_o^2 \geq -3\sigma(F_o^2)$)	0.992 ($F_o^2 \geq -3\sigma(F_o^2)$)

[a] Cell parameters obtained from least-squares refinement of 7413 centered reflections. [b] Cell parameters obtained from least-squares refinement of 5538 centered reflections. [c] Cell parameters obtained from least-squares refinement of 7146 centered reflections. [d] An idealized gemetry was imposed upon the disordered tetrafluoroborate ion and solvent dichloromethane molecule through imposition of idealized F−B (1.36 Å), F···F (2.22 Å), Cl−C (1.80 Å), and Cl···Cl (2.95 Å) distances. [e] $R_1 = \sum||F_o| - |F_c||/\sum|F_o|$; $wR_2 = [\sum w(F_o^2 - F_c^2)^2/\sum w(F_o^4)]^{1/2}$ [f] $S = [\sum w(F_o^2 - F_c^2)^2/(n - p)]^{1/2}$ (n = number of data, p = number of parameters varied; $w = [\sigma^2(F_o^2) + (a_0 P)^2 + a_1 P]^{-1}$, where $P = [\max(F_o^2, 0) = 2F_c^2]/3$. For **4**, a_0 = 0.0485 and a_1 = 13.904. For **5**, a_0 = 0.0467 and a_1 = 0.00. For **8b**, a_0 = 0.0904 and a_1 = 0.00.

Scheme 1

X$^-$ = CF$_3$SO$_3^-$
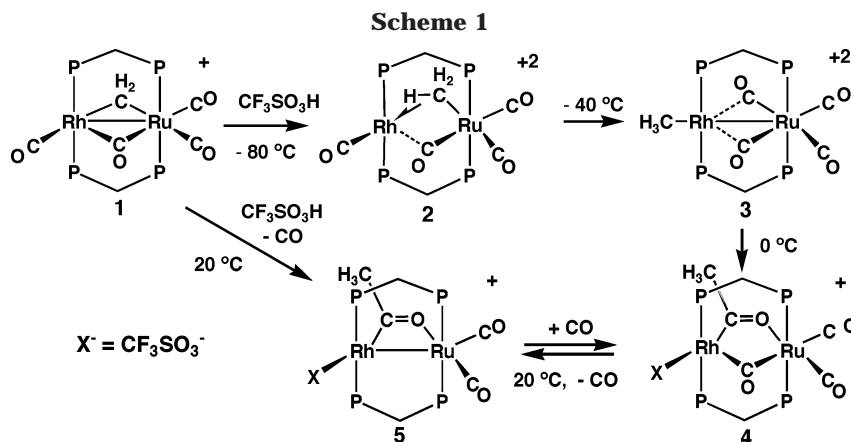
20% greater than those of the attached carbons. The final model for **4** was refined to values of $R_1(F)$ = 0.0393 (for 10 496 data with $F_o^2 \geq 2\sigma(F_o^2)$) and $wR_2(F^2)$ = 0.1076 (for all 11 881 data).

The structure for **5** was solved and refined as described for compound **4**, using similar hydrogen atom location procedures. The final model was refined to values of $R_1(F)$ = 0.0488 (for 8659 data with $F_o^2 \geq 2\sigma(F_o^2)$) and $wR_2(F^2)$ = 0.1083 (for all 12 368 data).

The structure for **8b** was solved using direct methods (SHELXS-86),)[20] and refinement was completed as for **4** and **5** above. The final model was refined to values of $R_1(F)$ = 0.0571 (for 7085 data with $F_o^2 \geq 2\sigma(F_o^2)$) and $wR_2(F^2)$ = 0.1653 (for all 11 004 data).

(20) Sheldrick, G. M. *Acta Crystallogr., Sect. A* **1990**, *46*, 467.

Results and Compound Characterization

Protonation of the methylene-bridged compound [RhRu(CO)$_4$(μ-CH$_2$)(dppm)$_2$][CF$_3$SO$_3$] (**1**) at −80 °C using triflic acid affords the dicationic methyl compound [RhRu(CO)$_4$(μ-CH$_3$)(dppm)$_2$][CF$_3$SO$_3$]$_2$ (**2**), as diagrammed in Scheme 1. No other species was observed at this temperature. The ^{31}P{^{1}H} NMR spectrum of **2** contains two signals for the different ends of the diphosphine ligands at δ 24.2 and 20.8 with patterns typical of an AA′BB′X spin system found in similar Rh/M (M = Ru, Os) systems. The ^{1}H NMR spectrum of **2** displays two multiplets at δ 4.10 and 3.63 corresponding to the dppm methylene protons and a broad singlet integrating for three hydrogens at δ 0.30. Unfortunately, the close proximity of the two phosphorus signals in the ^{31}P{^{1}H}

NMR spectrum prevented use of selective $^1H\{^{31}P\}$ experiments to aid in determining the binding mode of the methyl ligand. In an analogous Rh/Os complex, also having a broad unresolved methyl signal, $^1H\{^{31}P\}$ selective decoupling experiments demonstrated coupling of these methyl protons to all four phosphorus nuclei, suggesting a bridging CH_3 group.

To examine the bonding involving the methyl group in this Rh/Ru species, isotopomers of **2** incorporating CH_2D, CD_2H, and $^{13}CH_3$ were prepared. The CH_2D isotopomer (**2**-CH_2D) was prepared by protonation of compound **1** with CF_3SO_3D, whereas the CD_2H isotopomer (as well as detectable amounts of the isotopomers CH_3 and CH_2D)[21] was synthesized by protonation of $[RhRu(CO)_4(\mu$-$CD_2)(dppm)_2][CF_3SO_3]$ (**1**-CD_2) with triflic acid. At -60 °C, the ^1H NMR spectrum displays the methyl resonance of **2** at δ 0.30, of **2**-CH_2D at δ 0.13, and of **2**-CD_2H at δ -0.09. The upfield shift of the protons of the bridging methyl group as the level of deuterium incorporation is increased is characteristic of an agostic interaction, in which the lower zero-point energy of the C–D bond relative to the C–H bond favors the C–H agostic interaction over agostic interactions involving the C–D bond. The NMR technique of observing changes in chemical shift with isotopic labeling is referred to as isotopic perturbation of resonance (IPR) and has been used to probe the nature of bridging and/or agostic methyl groups in transition-metal complexes, first by Shapley[22] and subsequently by others.[23–25] Further evidence supporting the agostic methyl interaction was obtained from the ^1H NMR spectrum of a $^{13}CH_3$-enriched sample of **2**. Although the observed one-bond carbon–hydrogen coupling of 127 Hz is within the accepted range for terminal methyl groups (120–145 Hz for typical late-metal complexes[26]), it is also close to the 121 Hz observed for the late-metal complexes $[Os_3$-$(CO)_{10}(\mu$-$H)(\mu$-$CH_3)]$[22] and $[Cp_2Fe_2(CO)_2(\mu$-$CH_3)(\mu$-$CO)]$[25a] and to the value of 125 Hz for the Rh/Os analogue $[RhOs(CO)_4(\mu$-$CH_3)(dppm)_2][CF_3SO_3]_2$,[12c] all of which have previously been shown by IPR techniques to possess bridging agostic methyl groups. In addition, the value of 127 Hz is significantly smaller than the one-bond coupling observed for complex **3** (139 Hz), in which the methyl group is terminally bound (vide infra). Assuming the two terminal C–H bonds have one-bond coupling of near 140 Hz, we can estimate the coupling constant for the agostic C–H bond from the weighted average given above as 101 Hz—a value that is typical for such interactions.[24,27] On the basis of the C–H coupling constant and the IPR experiments we conclude

that the methyl group bridges both metals, being σ-bound to one and involved in an agostic interaction with the other.

The $^{13}C\{^1H\}$ NMR spectrum of **2** at -80 °C shows the methyl signal as a sharp singlet at δ -20.7 with no apparent coupling to either the ^{103}Rh or ^{31}P nuclei. The absence of Rh coupling establishes that this group is σ-bound to Ru and presumably indicates a relatively weak agostic contact with Rh. The high-field chemical shift of this carbon is also in line with that observed for the analogous Rh/Os methyl complex (δ -32.2). In the carbonyl region, two broad signals, observed at δ 190.4 and 187.7, are assigned as terminally bound to Ru, due to the lack of any observable Rh coupling, whereas the resonance appearing as a doublet of triplets at δ 183.4 is assigned as a terminal Rh-bound carbonyl ($^1J_{RhC} = 79$ Hz, $^2J_{P(Rh)C} = 15$ Hz). A fourth signal, at δ 219.5, is assigned as a Ru-bound semibridging carbonyl. The low-field shift of this carbon is suggestive of a semibridging interaction, although the lack of Rh coupling indicates that the interaction with this metal must be weak.

When a solution of **2** is warmed to -40 °C, a new compound, $[RhRu(CO)_4(CH_3)(dppm)_2][CF_3SO_3]_2$ (**3**), is formed, which is an isomer of **2**, in which the formerly Ru-bound agostic methyl group is now terminally bound to Rh. The ^1H NMR spectrum of **3** shows one broad multiplet at δ 3.41, assigned to the four equivalent dppm methylene protons, indicating front–back symmetry of the complex, in which the environment on one side of the $RhRuP_4$ plane is equivalent to that on the other. The remaining proton signal at δ 1.66 appears as a triplet of doublets due to coupling to Rh ($^2J_{RhH} = 4$ Hz) and to the Rh ends of the diphosphine ligands ($^3J_{PH} = 8$ Hz). A ^1H NMR experiment using a $^{13}CH_3$-enriched sample of **3** displays a one-bond C–H coupling of 139 Hz, consistent with a terminally bound methyl group. The $^{13}C\{^1H\}$ NMR spectrum of **3** shows two broad, unresolved signals in the carbonyl region at δ 186.3 and 221.6, corresponding to the pair of chemically equivalent terminally bound carbonyls on Ru and the two semibridging CO ligands, respectively. The low-field chemical shift of the second signal establishes that it is bridging, and the lack of resolvable Rh coupling indicates that it is primarily bound to Ru and has a weak interaction with Rh. The methyl carbon appears as a doublet at δ 42.2 ($^1J_{RhC} = 25$ Hz), shifted considerably downfield from that of the methyl group in the precursor **2**.

Further warming to 0 °C causes **3** to transform into a third compound, $[RhRu(OSO_2CF_3)(CO)_3(\mu$-$C(CH_3)O)$-$(dppm)_2][CF_3SO_3]$ (**4**). In the ^1H NMR spectrum two resonances appear for the dppm methylene protons, indicating that the "front–back" symmetry of the precursor (**3**) is broken, and the methyl resonance now appears as a broad singlet at δ 2.03, with no obvious coupling to either ^{103}Rh or ^{31}P. In addition, when the sample is ^{13}CO-enriched, the methyl proton signal broadens noticeably, although the additional coupling is not resolved. These data suggest an acyl formulation for compound **4**, which is further supported by the $^{13}C\{^1H\}$ NMR spectrum of a ^{13}CO-enriched sample that displays a low-field resonance at δ 304.8 showing strong coupling to Rh ($^1J_{RhC} = 38$ Hz). This very low field chemical shift for the acyl carbon has been observed

(21) The presence of the different isotopomers of **2** arose due to adventitious water in the CF_3SO_3D before protonation of **1** and due to small amounts of **1** amd **1**-CHD present in the sample of **1**-CD_2.

(22) Calvert, R. B.; Shapley, J. R. *J. Am. Chem. Soc.* **1978**, *100*, 7726.

(23) Brookhart, M.; Green, M. L. H.; Wong, L. L. *Prog. Inorg. Chem.* **1988**, *36*, 1.

(24) Dawkins, G. M.; Green, M.; Orpen, A. G.; Stone, F. G. A. *J. Chem. Soc., Chem. Commun.* **1982**, 41.

(25) (a) Casey, C. P.; Fagan, P. J.; Miles, W. H. *J. Am. Chem. Soc.* **1982**, *104*, 1134. (b) Green, M. L. H.; Hughes, A. K.; Popham, N. A.; Stephens, A. H. H.; Wong, L. L. *J. Chem. Soc., Dalton Trans.* **1992**, 3077.

(26) (a) Kulzick, M. A.; Price, R. T.; Andersen, R. A.; Muetterties, E. L. *J. Organomet. Chem.* **1987**, *333*, 105. (b) Siedle, A. R.; Newmark, R. A.; Pignolet, L. H. *Organometallics* **1984**, *3*, 855. (c) Haynes, A.; Mann, B. E.; Morris, G. E.; Maitlis, P. M. *J. Am. Chem. Soc.* **1993**, *115*, 4093.

(27) Crabtree, R. H.; Hamilton, D. G. *Adv. Organomet. Chem.* **1983**, *250*, 395.

Figure 1. Perspective view of the complex cation of [RhRu-$(OSO_2CF_3)(CO)_2(\mu$-C(CH$_3$)O)$(\mu$-CO)(dppm)$_2$][CF$_3$SO$_3$] (**4**) showing the atomic numbering scheme. Non-hydrogen atoms are represented by Gaussian ellipsoids at the 20% probability level. Hydrogen atoms are shown with arbitrarily small thermal parameters. Only the ipso carbons of the phenyl rings are shown.

previously in dmpm and/or dppm complexes of Rh/Rh,[28] Ru/Ru,[29,30] and Rh/Os[12c] and suggests a bridging acyl group having significant carbene-like character, not likely that of a terminal acyl moiety, which appears at much higher fields (δ 240−260).[28−31] Two additional carbonyl resonances appear at δ 196.6 and 184.9 and are clearly identified as Ru-bound on the basis that no Rh coupling is observed. The third carbonyl, at δ 250.3, appears as a complex multiplet and appears to correspond to a bridging carbonyl in which the coupling to Rh is unresolved from coupling to the four ^{31}P nuclei and the other carbonyls. The methyl group of the acyl moiety appears as a broad singlet at δ 45.2.

The IR spectrum of **4** shows two terminal carbonyl bands at 2090 and 2016 cm^{-1} and a bridging carbonyl at 1732 cm^{-1}, but no stretch for the acyl carbonyl was observed, even for a ^{13}CO-enriched sample. The acyl carbonyl stretch in the IR spectrum was also absent in other related binuclear acetyl-bridged complexes containing similar metals,[29,30] although it was identified at 1485 cm^{-1} in the dirhodium system.[28]

The structural assignment for **4** has been confirmed by an X-ray determination, for which the cation is diagrammed in Figure 1 (with relevant bond lengths and angles given in Table 3). It is immediately evident that migration of the methyl ligand to a carbonyl has occurred and that the resulting bridging acyl group is carbon-bound to Rh and oxygen-bound to Ru. The Rh−C(4) bond of the bridging acyl group (1.924(3) Å) is significantly shorter than that reported by Eisenberg (2.05(2) Å) for a related Rh$_2$ system; however, the C(4)−O(4) acyl distance in **4** (1.243(4) Å) is comparable to that for the Rh$_2$ system (1.28(2) Å).[28] The present C−O distance is somewhat longer than the typical distances in aldehydes and ketones (between 1.19 and 1.23 Å) but still much shorter than C−O single bonds in enols (ca. 1.33 Å).[32] All the angles at the acyl carbon (C(4)) are close to the idealized value for sp^2 hybridization.

(28) Shafiq, F.; Kramarz, K. W.; Eisenberg, R. *Inorg. Chim. Acta* **1993**, *213*, 111.
(29) Gao, Y.; Jennings, M. C.; Puddephatt, R. J. *Organometallics* **2001**, *20*, 1882.
(30) Johnson, K. A.; Gladfelter, W. L. *Organometallics* **1990**, *9*, 2101.
(31) Jeffery, J. C.; Orpen, A. G.; Stone, F. G. A.; Went, M. J. *J. Chem. Soc., Dalton Trans.* **1986**, 173.
(32) Allen, F. H.; Kennard, O.; Watson, D. G.; Brammer, L.; Orpen, A. G.; Taylor, R. *J. Chem. Soc., Perkin Trans. 2* **1987**, S1.

Table 3. Selected Distances and Angles for Compound 4

Distances (Å)			
Rh−Ru	3.3992(4)[a]	Ru−C(2)	1.865(3)
Rh−P(1)	2.3691(8)	Ru−C(3)	1.991(3)
Rh−P(3A)[b]	2.34(2)	P(1)−P(2)	3.132(1)[a]
Rh−P(3B)[b]	2.40(2)	P(3A)−P(4)	3.16(2)[a]
Rh−O(5)	2.241(3)	P(3B)−P(4)	3.10(2)[a]
Rh−C(1)	2.011(3)	O(1)−C(1)	1.190(4)
Rh−C(4)	1.924(3)	O(2)−C(2)	1.137(4)
Ru−P(2)	2.3895(8)	O(3)−C(3)	1.117(4)
Ru−P(4)	2.3995(8)	O(4)−C(4)	1.243(4)
Ru−O(4)	2.114(2)	C(4)−C(5)	1.502(5)
Ru−C(1)	2.068(3)		

Angles (deg)			
P(1)−Rh−P(3A)	173.8(6)	C(2)−Ru−C(3)	90.3(1)
P(1)−Rh−P(3B)	169.2(6)	Ru−O(4)−C(4)	120.1(2)
O(5)−Rh−C(1)	106.3(1)	Rh−O(5)−S(1)	166.9(2)
O(5)−Rh−C(4)	159.7(1)	Rh−C(1)−Ru	112.9(1)
C(1)−Rh−C(4)	93.8(1)	Rh−C(1)−O(1)	113.8(2)
P(2)−Ru−P(4)	171.42(3)	Ru−C(1)−O(1)	133.3(2)
O(4)−Ru−C(1)	88.8(1)	Ru−C(2)−O(2)	176.8(3)
O(4)−Ru−C(2)	176.7(1)	Ru−C(3)−O(3)	178.9(3)
O(4)−Ru−C(3)	86.6(1)	Rh−C(4)−O(4)	124.4(2)
C(1)−Ru−C(2)	94.3(1)	Rh−C(4)−C(5)	119.1(3)
C(1)−Ru−C(3)	175.4(1)	O(4)−C(4)−C(5)	116.5(3)

[a] Nonbonded distance. [b] P(3) is disordered over two sites. See Experimental Section for details.

The Rh−Ru separation of 3.3992(4) Å is significantly longer than the intraligand P−P distances (3.132(1) and 3.16(2)/3.10(2) Å for the disordered P(3)) and indicates that no metal−metal bond is present. This large metal−metal separation leads to a Rh−C(1)−Ru angle of 112.9(1)°, suggesting sp^2 hybridization of this carbonyl carbon, and the C(1)−O(1) distance (1.190(4) Å) as a result is substantially longer than those of the terminal carbonyls, although not quite as long as that of the bridging acyl group. As noted earlier, this distance compares favorably with C=O bonds in aldehydes and ketones. The bond angles around C(1) display a large asymmetry in the bridging carbonyl (Rh−C(1)−O(1) = 113.8(2)° and Ru−C(1)−O(1) = 133.3(2)°).

Figure 1 also clearly shows that one of the triflate ions is coordinating to Rh, directly opposite the acyl group (C(4)−Rh−O(5) = 159.7(1)°), with a normal Rh−O(5) distance of 2.241(3) Å.[33] It is assumed that this structure is maintained in solution, in order for Rh to maintain a 16-electron configuration. Displacement of the triflate ion by solvent is ruled out by the essentially unchanged spectral parameters in different solvents (CD$_2$Cl$_2$ and acetone-d_6). In addition, the IR spectrum of **4** in CH$_2$Cl$_2$ solution shows a strong band at 1265 cm^{-1}, suggesting the presence of a coordinated triflate ion.[34] The single ^{19}F resonance observed over a range of temperatures in the ^{19}F NMR spectrum indicates either facile exchange of free and coordinated triflate ion or the accidental equivalence of the chemical shifts for the two groups.

The above X-ray and spectroscopic data are both consistent with a significant degree of carbene-like character,[35,36] as diagrammed in structure **B** in Chart 1, leading us to favor the oxycarbene formulation of this

(33) Orpen, A. G.; Brammer, L.; Allen, F. H.; Kennard, O.; Watson, D. G.; Taylor, R. *J. Chem. Soc., Dalton Trans.* **1989**, 51.
(34) Lawrance, G. A. *Chem. Rev.* **1986**, *86*, 17.
(35) Erker, G. *Angew. Chem., Int. Ed. Engl.* **1989**, *28*, 397.
(36) Schubert, U. *Coord. Chem. Rev.* **1984**, *55*, 261.

Chart 1

Figure 2. Perspective view of the complex cation of [RhRu-$(OSO_2CF_3)(CO)_2(\mu$-C(CH$_3$)O)(dppm)$_2$][CF$_3$SO$_3$] (**5**). Thermal parameters are as described in Figure 1.

bridging ligand, over the more conventional acyl formulation (**A**).

If a solution of compound **4** is purged with argon, or exposed to vacuum, at ambient or higher temperatures, quantitative conversion to a new compound is observed in the ^{31}P{^{1}H} NMR spectrum within minutes. This compound can also be obtained by direct treatment of **1** with triflic acid at ambient temperature. Complex **4** can be regenerated upon exposure of this new species to CO. The ^{1}H NMR spectrum of this new complex contains a singlet at δ 1.99, indicative of the methyl group of an acyl moiety, and the ^{13}C{^{1}H} NMR spectrum of a ^{13}CO-enriched sample reveals the presence of two terminal carbonyls at δ 204.2 and 180.4 that display no coupling to Rh and a low-field doublet resonance at δ 270.3 displaying 33 Hz coupling to Rh. These data are supportive of a dicarbonyl species with the acetyl group remaining intact and being carbon-bound to Rh and, thus, is formulated as [RhRu(OSO$_2$CF$_3$)(CO)$_2$(μ-C(CH$_3$)-O)(dppm)$_2$][CF$_3$SO$_3$] (**5**). The IR spectrum displays two terminal carbonyl stretches at 2045 and 1989 cm^{-1}, and once again no acyl stretch is obvious.

The structure of **5** was also confirmed by an X-ray determination, and the cation is shown in Figure 2 with relevant bond lengths and angles given in Table 4. The obvious differences between the structures for compounds **4** and **5** are the absence of a bridging carbonyl in the latter and the substantial compression of the Rh–Ru distance compared to **4** (2.6953(4) vs 3.3992(4) Å), to a value that is typical for a single bond involving these metals. As with **4**, the bond lengths within the acyl group suggest significant carbene character (Rh–C(3) = 1.912(4) Å and C(3)–O(3) = 1.266(5) Å). In this case, the acyl C(3)–O(3) distance is elongated compared to that in compound **4** and is now intermediate between the double bond of aldehydes (1.19 Å) and the single

Table 4. Selected Distances and Angles for Compound 5

Distances (Å)			
Rh–Ru	2.6953(4)	Ru–C(1)	1.877(5)
Rh–P(1)	2.333(1)	Ru–C(2)	1.898(4)
Rh–P(3)	2.332 (1)	P(1)–P(2)	2.98(1)^a
Rh–O(4)	2.219(3)	P(3)–P(4)	2.98(1)^a
Rh–C(3)	1.912(4)	O(1)–C(1)	1.138(5)
Ru–P(2)	2.409(1)	O(2)–C(2)	1.127(5)
Ru–P(4)	2.412(1)	O(3)–C(3)	1.266(5)
Ru–O(3)	2.146(3)	C(3)–C(4)	1.510(6)

Angles (deg)			
Ru–Rh–P(1)	93.44(3)	P(2)–Ru–P(4)	165.21(4)
Ru–Rh–P(3)	93.57(3)	O(3)–Ru–C(1)	157.4(1)
Ru–Rh–O(4)	109.57(8)	O(3)–Ru–C(2)	107.8(2)
Ru–Rh–C(3)	68.88(12)	C(1)–Ru–C(2)	94.8(2)
P(1)–Rh–P(3)	167.45(4)	Ru–O(3)–C(3)	100.6(2)
O(4)–Rh–C(3)	178.3(1)	Rh–O(4)–S(1)	131.2(2)
Rh–Ru–P(2)	93.39(3)	Ru–C(1)–O(1)	175.6(4)
Rh–Ru–P(4)	93.27(3)	Ru–C(2)–O(2)	176.0(4)
Rh–Ru–O(3)	69.27(7)	Rh–C(3)–O(3)	121.3(3)
Rh–Ru–C(1)	88.1(1)	Rh–C(3)–C(4)	123.6(3)
Rh–Ru–C(2)	177.1(1)	O(3)–C(3)–C(4)	115.1(4)

^{a} Nonbonded distance.

Chart 2
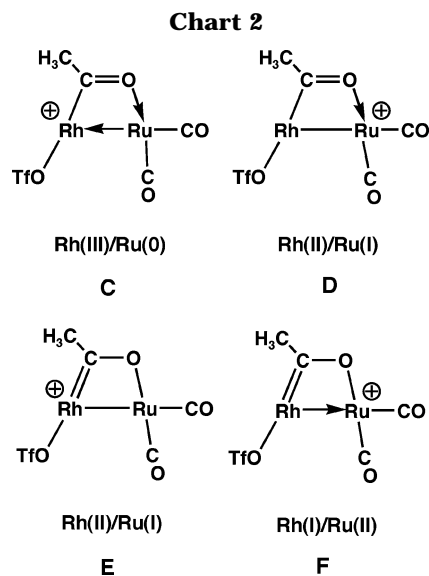
bond in enols (1.33 A).^{32} Although the dramatic change in metal–metal separation on removal of a carbonyl from **4** has had little effect on the parameters within the acyl group, it has resulted in a significant compression of the C(3)–O(3)–Ru angle from 120.1(2) to 100.6(2)°.

The bonding within the RhRu(μ-C(CH$_3$)O) framework and the accompanying oxidation states of the metals are equivocal, and limiting valence-bond formulations are shown in Chart 2. If one considers a normal acetyl bonding mode, shown in structures **C** and **D**, the oxidation states can be either Rh^{3+}/Ru^0, in which the positive charge on the complex is localized on Rh, which achieves a 16e configuration by dative bond formation from Ru^0 (structure **C**), or **D**, in which the oxidation states are Rh^{2+}/Ru$^+$. In this latter model the positive charge now resides on Ru and a conventional metal–metal bond results, again giving the favored 16e/18e configurations at the metals. The other formulation, represented by structures **E** and **F**, invokes the oxy–carbene bonding scheme, in which the oxidation states of the two metals can be either Rh^{2+}/Ru$^+$ (**E**) or Rh$^+$/Ru^{2+} (**F**). The solid-state structure and ^{13}C NMR experi-

Scheme 2

Scheme 3

X = CF$_3$SO$_3$ (**7a**), BF$_4$ (**7b**)
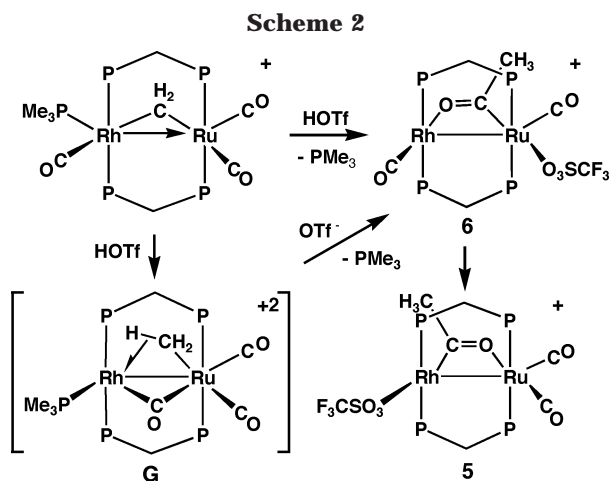
ments suggest substantial contribution from the oxy–carbene formulations, and that involving the Rh$^+$/Ru^{2+} oxidation states (structure **F**) is preferred on the basis that these are common oxidation states observed for these metals.

It is important to note that substitution of the triflate anion for fluoroborate anion by protonation of [RhRu-(CO)$_4$(μ-CH$_2$)(dppm)$_2$][BF$_4$] with HBF$_4$ does not give the BF$_4^-$-coordinated analogues to compounds **4** or **5**. Instead, decomposition into a complex mixture of products results. Apparently the BF$_4^-$ anion is too weakly coordinating[37] to stabilize these acyl complexes. This observation offers additional support for the coordination of the triflate anion in solutions of **4** and **5**, as discussed earlier.

Protonation of the PMe$_3$ adduct [RhRu(CO)$_3$(PMe$_3$)-(μ-CH$_2$)(dppm)$_2$]$^+$, which is isoelectronic with the methylene-bridged tetracarbonyl species **1**, using a slight excess of triflic acid gives quantitative conversion to a new complex, [Rh*Ru*(OSO$_2$CF$_3$)(CO)$_2$(μ-C(CH$_3$)O)-(dppm)$_2$][CF$_3$SO$_3$] (**6**), as shown in Scheme 2; free PMe$_3$ and HPMe$_3^+$, the latter resulting from protonation of the phosphine by excess acid, are also observed. No additional species was observed upon protonation of the precursor at −80 °C. The acyl product **6** is an isomer of **5**, in which the bridging acyl group is now carbon-bound to Ru. This new isomer displays a singlet for the acetyl methyl group in the ^{1}H NMR spectrum at δ 1.93, and the ^{13}C{^{1}H} NMR spectrum of a ^{13}CO-enriched sample displays three carbonyl resonances. A triplet at δ 196.3 and a doublet of triplets at δ 186.8 ($^1J_{RhC}$ = 75 Hz) indicate that there is one terminal carbonyl on each metal, and the low-field resonance at δ 293.3 is a broad singlet, with no resolvable coupling to Rh, suggesting an acyl group that is now carbon-bound to Ru. To maintain the electron count, the triflate anion must now also be on Ru, giving this metal an 18-electron configuration. The IR spectrum displays two terminal CO bands at 2015 and 1956 cm^{-1}, with no observable stretch for the acyl group or the ν_{SO} band of the coordinated triflate group. Complex **6** is unstable in solution, converting to the original isomer **5** within a few hours.

An analogous rearrangement of the acyl group has also been observed in the RhOs system, in which treatment of the RhOs analogue of **4**, [RhOs(OSO$_2$CF$_3$)-
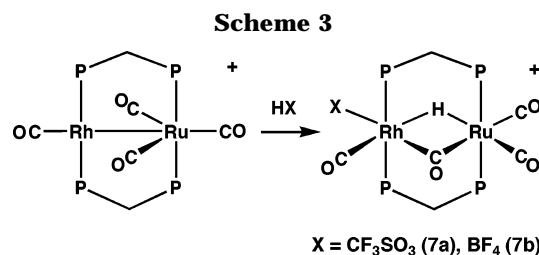
(CO)$_3$(μ-C(CH$_3$)O)(dppm)$_2$][CF$_3$SO$_3$], with PMe$_3$ at room temperature afforded the dicationic acyl complex [Rh*Os*-(PMe$_3$)(CO)$_3$(μ-C(CH$_3$)O)(dppm)$_2$][CF$_3$SO$_3$]$_2$, in which the acyl carbon is bound to Os.[12c] Unfortunately, the reactions of compounds **4** and **5** with PMe$_3$ do not yield tractable products, instead giving a complex mixture of several products, none of which could be isolated or properly characterized due to overlap of multiple signals in both the ^{31}P{^{1}H} and ^{1}H NMR spectra.

An attempt was made to generate methyl complexes and ultimately the acyl-bridged species **4** and **5** in a reverse order, by reaction of an appropriate hydride species with diazomethane. The precursor hydride complexes [RhRu(X)(μ-H)(CO)$_4$(dppm)$_2$][X] (X = CF$_3$SO$_3$ (**7a**), BF$_4$ (**7b**)) were obtained by protonation of [RhRu-(CO)$_4$(dppm)$_2$][X], as shown in Scheme 3. For complex **7a**, the hydride resonance appears as a complex multiplet at δ −10.41 in the ^{1}H NMR spectrum; for **7b**, the hydride appears at δ −11.07. Upon broad-band ^{31}P decoupling, the hydride resonance in each case simplifies to a doublet with coupling to Rh of 19 Hz. The selective ^{31}P decoupling experiments necessary for extracting the coupling of the hydride ligands to each of the two sets of ^{31}P nuclei could not be carried out, owing to the close proximity of these two resonances in the ^{31}P{^{1}H} NMR spectrum, preventing us from gaining better information regarding the exact nature of the hydride bonding. The IR spectrum of **7a** shows four carbonyl bands, with three terminal stretches at 2072, 2040, and 1999 cm^{-1}. The fourth band is at slightly lower frequency (1880 cm^{-1}), suggesting a bridging interaction, and a stretch at 1284 cm^{-1} suggests triflate ion coordination.

Neither complex **7a** nor **7b** reacts with diazomethane, even after several days; therefore, the targeted methyl species leading to an acyl product could not be obtained by this route. Although diazomethane insertion into metal–ligand bonds is well established,[38] including into metal–hydride bonds,[38g,39] we have observed no clear examples of CH$_2$ insertions into metal–hydride bonds in these and related species.[12c]
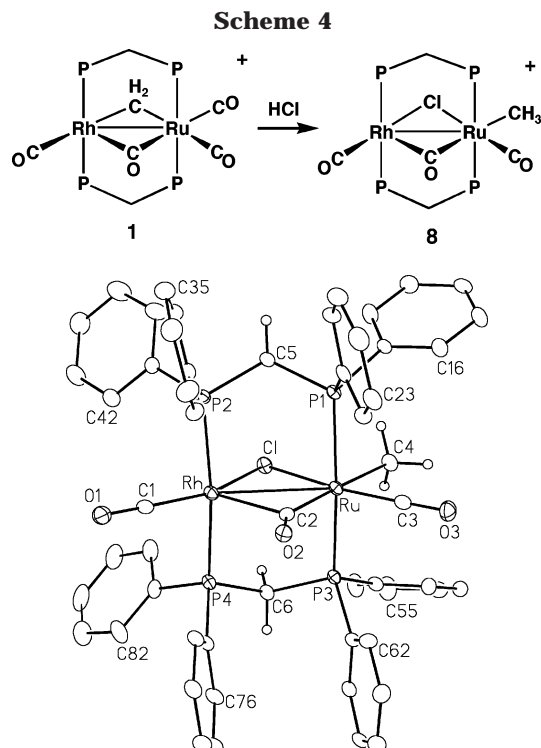
Unlike the reaction with triflic acid, protonation of **1** with HCl does not yield an acyl complex. Instead the

(37) Beck, W.; Sunkel, K. *Chem. Rev.* **1988**, *88*, 1405.

(38) (a) Seyferth, D. *Chem. Rev.* **1955**, *55*, 1155. (b) Mango, F.; Dvoretzky, I. *J. Am. Chem. Soc.* **1966**, *88*, 1654. (c) Thorn, D. L.; Tulip, T. H. *J. Am. Chem. Soc.* **1981**, *103*, 5984. (d) Kleitzein, H.; Werner, H.; Serhadli, P.; Ziegler, M. L. *Angew. Chem., Int. Ed. Engl.* **1983**, *22*, 46. (e) Jernakoff, P.; Cooper, N. J. *J. Am. Chem. Soc.* **1984**, *106*, 3026. (f) Lisko, J. R.; Jones, W. M. *Organometallics* **1985**, *4*, 944. (g) Azam, K. A.; Frew, A. A.; Lloyd, B. R.; Manojlovic-Muir, Lj.; Muir, K. W.; Puddephatt, R. J. *Organometallics* **1985**, *4*, 1400. (h) Stenstrøm, Y.; Jones, W. M. *Organometallics* **1986**, *5*, 178. (i) Stenstrøm, Y.; Klauck, G.; Koziol, A.; Palenik, G. J.; Jones, W. M. *Organometallics* **1986**, *5*, 2155.

(39) (a) Empsall, H. D.; Hyde, E. M.; Markham, M.; McDonald, W. S.; Norton, M. C.; Shaw, B. L.; Weeks, B. *J. Chem. Soc., Chem. Commun.* **1971**, 589. (b) Calvert, R. G.; Shapley, J. R. *J. Am. Chem. Soc.* **1977**, *99*, 5225. (c) Hamilton, D. H.; Shapley, J. R. *Organometallics* **2000**, *19*, 761. (d) Kabir, S. E.; Malik, K. M. A.; Mandal, H. S.; Mottalib, M. A.; Abedin, M. J.; Rosenberg, E. *Organometallics* **2002**, *21*, 2593.

Scheme 4

Figure 3. Perspective view of the complex cation of [RhRu-(CH$_3$)(CO)$_2$(μ-Cl)(μ-CO)(dppm)$_2$][CF$_3$SO$_3$] (**8b**). Thermal parameters are as described in Figure 1. All carbon atoms of the phenyl rings are shown, but the phenyl hydrogens are omitted.

methyl complex [RhRu(CH$_3$)(CO)$_2$(μ-Cl)(μ-CO)(dppm)$_2$]-[CF$_3$SO$_3$] (**8a**) is formed, as shown in Scheme 4. The ^{1}H NMR spectrum shows a triplet at high field (δ -0.21) typical of a metal-bound methyl group. The IR spectrum of this new compound contains two terminal carbonyl bands at 2013 and 1986 cm^{-1}, as well as what appears to be a bridging CO stretch at 1711 cm^{-1}. The ^{13}C{^{1}H} NMR spectrum of a ^{13}CO-enriched sample of **8a** shows three resonances in the carbonyl region; a low-field signal at δ 246.4 appears as a complex multiplet and can be assigned as a bridging or semibridging carbonyl showing unresolved coupling to Rh and to both ends of the diphosphines, while the remaining two resonances appear at δ 199.4 (triplet) and 188.8 (doublet of triplets, $^1J_{\text{RhC}}$ = 76 Hz) and are assigned to the terminally bound carbonyls on Ru and Rh, respectively.

The structure of compound **8b** was established by an X-ray determination, and a representation of the complex cation is shown in Figure 3. Relevant bond lengths and angles are depicted in Table 5. Unlike the previous triflate species, in which the triflate ion is coordinated in a terminal site on one metal, the chloride anion in **8b** bridges both metals. The bridging carbonyl in **8b** appears to be semibridging and is more strongly bound to Ru than it is to Rh (Ru$-$C(2) = 2.056(6) Å, Rh$-$C(2) = 2.249(6) Å). In addition, this carbonyl is more linear with respect to Ru (Ru$-$C(2)$-$O(2) = 148.3(5)°, Rh$-$C(2)$-$O(2) = 123.0(5)°). The nature of the metal$-$metal interaction is not clear on the basis of the separation (3.0115(7) Å). Although this separation is significantly longer than normal for a single bond (cf. compound **2**), it is shorter than the intraligand P$-$P separations of 3.082(2) and 3.098(2) Å, suggesting some mutual attraction of the metals. Certainly, the metals may be

Table 5. Selected Distances and Angles for Compound 8b

Distances (Å)			
Rh$-$Ru	3.0115(7)	Ru$-$C(2)	2.056(6)
Rh$-$Cl	2.446(2)	Ru$-$C(3)	1.824(7)
Rh$-$P(2)	2.337(2)	Ru$-$C(4)	2.180(6)
Rh$-$P(4)	2.330(2)	P(1)$-$P(2)	3.082(2)^a
Rh$-$C(1)	1.827(7)	P(3)$-$P(4)	3.098(2)^a
Rh$-$C(2)	2.249(6)	O(1)$-$C(1)	1.131(7)
Ru$-$Cl	2.480(2)	O(2)$-$C(2)	1.141(7)
Ru$-$P(1)	2.395(2)	O(3)$-$C(3)	1.150(7)
Ru$-$P(3)	2.392(2)		

Angles (deg)			
Ru$-$Rh$-$Cl	52.83(4)	Rh$-$Ru$-$C(4)	135.9(2)
Ru$-$Rh$-$P(2)	93.14(4)	Cl$-$Ru$-$P(1)	88.59(5)
Ru$-$Rh$-$P(4)	92.22(4)	Cl$-$Ru$-$P(3)	86.50(5)
Ru$-$Rh$-$C(1)	151.4(2)	Cl$-$Ru$-$C(2)	100.1(2)
Ru$-$Rh$-$C(2)	43.0(2)	Cl$-$Ru$-$C(3)	167.1(2)
Cl$-$Rh$-$P(2)	85.97(5)	Cl$-$Ru$-$C(4)	84.1(2)
Cl$-$Rh$-$P(4)	90.21(5)	P(1)$-$Ru$-$P(3)	174.86(6)
Cl$-$Rh$-$C(1)	155.8(2)	C(2)$-$Ru$-$C(3)	92.8(3)
Cl$-$Rh$-$C(2)	95.8(2)	C(2)$-$Ru$-$C(4)	175.7(2)
P(2)$-$Rh$-$P(4)	169.62(6)	C(3)$-$Ru$-$C(4)	83.0(3)
C(1)$-$Rh$-$C(2)	108.4(3)	Rh$-$Cl$-$Ru	75.37(4)
Rh$-$Ru$-$Cl	51.81(4)	Rh$-$C(1)$-$O(1)	178.0(7)
Rh$-$Ru$-$P(1)	88.30(4)	Rh$-$C(2)$-$Ru	88.7(2)
Rh$-$Ru$-$P(3)	89.85(4)	Rh$-$C(2)$-$O(2)	123.0(5)
Rh$-$Ru$-$C(2)	48.3(2)	Ru$-$C(2)$-$O(2)	148.3(5)
Rh$-$Ru$-$C(3)	141.1(2)	Ru$-$C(3)$-$O(3)	176.1(6)

^{a} Nonbonded distance.

Chart 3
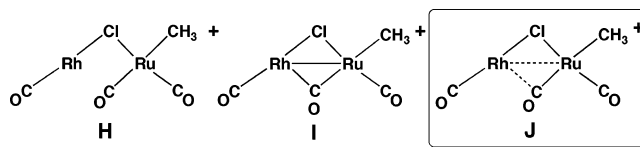
drawn together indirectly by their interactions with the semibridging carbonyl and the bridging chloro ligand. However, it is also useful to consider two bonding extremes for this compound, as shown in Chart 3. In structure **H** there is no metal$-$metal bond and all carbonyls are terminal, whereas in the other extreme (**I**) a metal$-$metal bond is accompanied by a conventional bridging carbonyl. The intermediate structure **J**, in which a weak interaction of Rh with the semibridging carbonyl is accompanied by some degree of metal$-$metal interaction, is not unlike that observed in the structure determination of **8b** as described above.

Discussion

Protonaton of the methylene-bridged species [RhRu-(CO)$_4$(μ-CH$_2$)(dppm)$_2$][CF$_3$SO$_3$] (**1**) at -80 °C using triflic acid gives the dicationic methyl complex [RhRu(CO)$_4$-(μ-CH$_3$)(dppm)$_2$][CF$_3$SO$_3$]$_2$ (**2**), in which the methyl group is asymmetrically bridging, being σ-bound to Ru and having an agostic interaction with Rh. The agostic interaction is presumably necessary to help alleviate the electron deficiency in this dicationic species and to give Rh a 16e configuration. Whether protonation has occurred directly at the bridging methylene group or at one of the metals, followed by migration to the methylene, is not known, although no hydrido species is observed at the lowest temperature studied.

When a solution of **2** is warmed to -40 °C, migration of the methyl group from the bridging position to a terminal site on Rh occurs, accompanied by a partial

Scheme 5
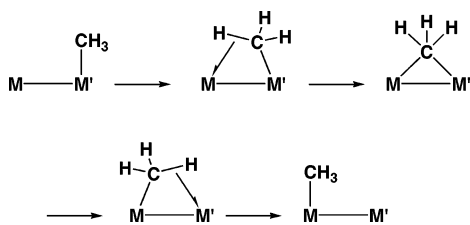
"merry-go-round" movement of the carbonyls, yielding **3**. Migration of methyl groups over a metal surface is a facile process,[40] and the transformation of **2** to **3** suggests how this might occur by modeling part of this migration. A terminally bound methyl group on one metal can initiate a weak interaction with an adjacent metal through an asymmetrical bridging interaction of the type observed in **2**, as diagrammed in Scheme 5. Further movement toward the second metal would yield a symmetrically bridged methyl group, examples of which are known.[41] Additional movement in the same direction yields a new asymmetrically bridged methyl group, which is now σ-bound to the second metal. Translation to the second metal is complete by movement of the methyl group to a terminal site on this metal.

In the observed transformation of **2** to **3**, it is not clear what favors migration of the methyl from an asymmetric bridging position to a terminal site on Rh. There is presumably little difference in metal−ligand bond strengths between Rh and Ru;[42] therefore, we assume that replacement of the asymmetrically bridged methyl group by a semibridging carbonyl, as observed in **3**, is favorable.

Warming a sample of **3** to approximately 0 °C results in migratory insertion of the methyl and a carbonyl group, affording the acyl-bridged product [RhRu(OSO$_2$-CF$_3$)(CO)$_3$(μ-C(CH$_3$)O)(dppm)$_2$][CF$_3$SO$_3$] (**4**), with concomitant coordination of a triflate anion at Rh. The observation that migratory insertion occurs at Rh instead of at Ru is of fundamental interest in mixed-metal chemistry, in which one attempts to utilize the different properties of different metals to influence the reactivity. In the analogous Rh/Os system,[12c] the observation of migratory insertion at Rh was not surprising, given the greater bond strengths of the third-row metal[42,43] and their resulting lower tendency for migratory insertion at that metal.[44] However, with the two adjacent second-row metals (Rh, Ru), having comparable bond strengths, the relative tendencies for migratory insertion were not so obvious. Certainly, it is well established that Co and Rh have a strong tendency to undergo migratory insertions, as witnessed by their extensive use in carbonylation reactions.[3] Furthermore, a computational study[45] has confirmed that migratory insertion to give acyl groups occurs more readily for Rh than for Ru, and although these calculations were performed on systems having no ancillary ligands, it was suggested that the influence of additional ligands would be minimal and would not significantly affect the outcome. An additional factor favoring migratory insertion in compound **3** may be the bonding of the carbonyls. In a classic mononuclear alkyl carbonyl complex, migration of an alkyl group to a carbonyl results in bending of the carbonyl away from the migrating group in the transition state.[1b] We suggest that the semibridging arrangement of two carbonyls in **3**, immediately preceding the migration, facilitates the migration process, since interaction of these carbonyls with Rh causes them to bend away from the methyl group, resembling somewhat the three-centered transition state and lowering the activation energy.

The coordinating ability of the triflate anion is pivotal in the migratory insertion process, filling the coordination site vacated by the migrating methyl group. Use of the more weakly coordinating tetrafluoroborate anion, by protonation of the BF$_4^-$ salt of **1** by HBF$_4$, yields the methyl complexes **2** and **3** at the appropriate low temperatures. However, warming does not yield the acyl complex, instead resulting in decomposition. Apparently, the BF$_4^-$ anion is too weakly coordinating to stabilize the acyl product. On the other hand, the use of the strongly coordinating chloride ion also does not lead to acyl formation, since chloride coordination occurs at an early stage accompanied by carbonyl loss to give the chloro-bridged methyl complex [RhRu(CH$_3$)(CO)$_3$-(μ-Cl)(dppm)$_2$][CF$_3$SO$_3$] (**8a**). The strong tendency for the chloride ion to occupy the bridging site and in so doing donate an additional pair of electrons, does not allow the methyl group to migrate to Rh, preventing subsequent chemistry as shown for the triflate complex.

As noted, the bridging acyl groups, in both the tricarbonyl (**4**) and dicarbonyl (**5**) products, have substantial carbene character and are more appropriately viewed as oxycarbenes than conventional acyl groups. One wonders whether this bonding formulation will influence the chemistry of this group and result in reactivity differences compared to terminally bound acyl groups. In FT chemistry, for example, a currently desirable product is ethanol.[46] Although reaction of a complex containing a terminally bound acetyl group with hydrogen could yield ethanol if initial hydrogen transfer to the oxygen occurred to give a hydroxycarbene, it is more likely that reductive elimination of acetaldehyde will result, by hydrogen transfer to the acyl carbon. However, one can foresee that in the bridging geometry hydrogen transfer to the oxygen of an oxycarbene moiety could occur, yielding a hydroxycarbene and leading ultimately to ethanol. Unfortunately, complex **5** reacts very slowly with hydrogen,

(40) Muetterties, E. L. *Bull. Soc. Chim. Belg.* **1975**, *84*, 959.

(41) See for example: (a) Schmidt, G. F.; Muetterties, E. L.; Beno, M. A.; Williams, J. M. *Proc. Natl. Acad. Sci. U.S.A.* **1981**, *78*, 1318. (b) Kulzick, M. A.; Price, R. T.; Andersen, R. A.; Muetterties, E. L. *J. Organomet. Chem.* **1987**, *333*, 105. (c) Reinking, M. K.; Fanwick, P. E.; Kubiak, C. P. *Angew. Chem., Int. Ed. Engl.* **1989**, *28*, 1377. (d) Schwartz, D. J.; Ball, G. E.; Andersen, R. A. *J. Am. Chem. Soc.* **1995**, *117*, 6027. (e) Yu, Z.; Wittbrodt, J. M.; Heeg, M. J.; Schlegel, H. B.; Winter, C. H. *J. Am. Chem. Soc.* **2000**, *122*, 9338.

(42) (a) Armentrout, P. B. In *Bonding Energetics in Organometallic Compounds*; Marks, T. J., Ed.; American Chemical Society: Washington, DC, 1990; Chapter 2. (b) Ziegler, T.; Tschinke, V. In *Bonding Energetics in Organometallic Compounds*; Marks, T. J., Ed.; American Chemical Society: Washington, DC, 1990; Chapter 19.

(43) Ziegler, T.; Tschinke, V.; Ursenbach, C. *J. Am. Chem. Soc.* **1987**, *109*, 4825.

(44) George, R.; Andersen, J.-A. M.; Moss, J. R. *J. Organomet. Chem.* **1995**, *505*, 131.

(45) Blomberg, M. R. A.; Karlsson, C. A. M.; Siegbahn, P. E. M. *J. Phys. Chem.* **1993**, *97*, 9341.

(46) (a) Ichikawa, M.; Fukuoka, A.; Hriljac, J. A.; Shriver, D. F. *Inorg. Chem.* **1987**, *26*, 3643. (b) Fukuoka, A.; Rao, L.-F.; Ichikawa, M. *Catal. Today* **1989**, *6*, 55. (c) Ichikawa, M.; Fukuoka, A.; Kimura, T. *Proceedings of the 9th International Congress on Catalysis*; Calgary, Chemical Institute of Canada: Ottawa, Canada, 1988; Vol. 2, p 258.

yielding methane as the only detected organic product, presumably by "deinsertion" of the acyl carbonyl to give a methyl complex, which ultimately yields methane upon reaction with H_2.

Although the conversion of **3** to **4** clearly results from migratory insertion at Rh, we have evidence that migratory insertion can also occur at Ru under slightly modified conditions. As noted, protonation of the PMe_3 adduct $[RhRu(PMe_3)(CO)_3(\mu\text{-}CH_2)(dppm)_2][CF_3SO_3]$ yields the metastable "reverse acyl" $[Rh\mathit{Ru}(OSO_2CF_3)(CO)_2\text{-}(\mu\text{-}C(CH_3)O)(dppm)_2][CF_3SO_3]$ (**6**). Binding of the acyl carbon to Ru suggests that migratory insertion may have also occurred at this metal. We propose that protonation of the PMe_3 adduct yields the asymmetrically bridged methyl complex **G**, as diagrammed in Scheme 2. In the related Rh/Os system a series of complexes, $[RhOs(PR_3)(CO)_2(\mu\text{-}CH_3)(\mu\text{-}CO)(dppm)_2][CF_3SO_3]_2$, exactly analogous to **G**, have been isolated and characterized for a range of phosphine ligands.[47] At this time it is not clear why migration of the methyl ligand to Rh does not occur in either of these species (Rh/Ru or Rh/Os). Presumably, in the Rh/Ru species (**G**) the greater tendency of Ru to undergo migratory insertion compared to Os[44] results in migration of the Ru-bound methyl to a Ru-bound carbonyl. After the migratory insertion, coordination of the triflate anion occurs, followed by movement of the acyl group to the bridging site, and loss of PMe_3 gives rise to **6**, in which the acyl carbon is bound to Ru.

This "reverse acyl" geometry has interesting implications related to the potential for ethanol formation discussed above. In this series of compounds attack by H_2 will presumably occur at Rh, the site of unsaturation. Having an oxycarbene that is *oxygen bound* to Rh is an ideal arrangement for potential hydrogen transfer to oxygen, yielding a hydroxycarbene. Unfortunately, H_2 addition to any of these acyl-bridged complexes is slow and isomerization of the "reverse acyl" species to compound **5** occurs more readily than H_2 addition, yielding only methane from the "deinsertion" process noted earlier.

Conclusions

The use of bimetallic catalysts is based on the concept that the two different metals together perform the catalytic transformation better than either metal alone. Whether this occurs because each metal plays a different role in substrate activation or whether the metals together perform in some other cooperative manner in which one metal influences the reactivity of the other

is often not known, and no doubt, variations and combinations of both reactivity modes will be found in different systems. Well-defined heterobinuclear complexes can function as useful models, helping us to understand the differing roles of the different metals in selected transformations.

In this study, in which protonation of the bridging methylene group in $[RhRu(CO)_4(\mu\text{-}CH_2)(dppm)_2][CF_3SO_3]$ (**1**) yields a bridging acetyl group, a number of transformations are observed that model relevant processes occurring on metal surfaces. The facile migration of a methyl ligand from one metal to the other and the characterization of an asymmetrically bridged methyl intermediate lead to a better understanding of the migration of methyl and other alkyl groups over a metal surface and of the possible role of bridged "agostic" alkyls in such migrations.

The known proclivity of Rh for inducing migratory insertion of alkyl and carbonyl groups is consistent with our subsequent observation of carbonyl insertion occurring at Rh upon protonation of **1**. However, the observation of a metastable bridging acyl, in which the acyl carbon is bonded to Ru instead of Rh upon protonation of $[RhRu(PMe_3)(CO)_3(\mu\text{-}CH_2)(dppm)_2][CF_3SO_3]$, suggests that in this case carbonyl insertion occurs at Ru, demonstrating that subtle changes in the metal environments can give rise to unexpected reactivity changes.

Finally, we note the potential significance of bridging acetyl groups on a metal surface for the direct formation of ethanol rather than acetaldehyde upon reaction with H_2. The significant oxycarbene character observed in these bridging acyl groups suggests that hydrogen transfer may give rise to hydroxycarbenes, which can ultimately yield ethanol. Unfortunately, in our model system, reaction with H_2 is very slow and the reactive species appears to be a methyl complex resulting from carbonyl deinsertion, giving methane as the only hydrogenation product.

Supporting Information Available: Tables of X-ray experimental details, atomic coordinates, interatomic distances and angles, anisotropic thermal parameters, and hydrogen parameters for compounds **4**, **5**, and **8b**. This material is available free of charge via the Internet at http://pubs.acs.org.

OM040051V

(47) Wigginton, J. R.; Trepanier, S. J.; Ferguson, M. J.; McDonald, R.; Cowie, M. Manuscript in preparation.